Stochastic phase dynamics: Multiscale behavior and coherence measures

Na Yu, R. Kuske,* and Y. X. Li
Department of Math, University of British Columbia, Vancouver, British Columbia
(Received 30 March 2005; revised manuscript received 20 January 2006; published 23 May 2006)

A multiscale approach is used to derive stochastic amplitude and phase dynamics for a canonical noise-sensitive model exhibiting coherence resonance. Explicit expressions for the dependence on noise levels and model type are compared with computational coherence measures.

DOI: 10.1103/PhysRevE.73.056205 PACS number(s): 89.20.−a

I. INTRODUCTION

Autonomous stochastic resonance refers to the occurrence of coherent behaviors such as rhythmic oscillations at an optimal level of noise in a system that is quiescent without noise. Unlike ordinary stochastic resonance in which the detectability of a periodic input is maximized by an optimal noise level, in autonomous stochastic resonance the coherent oscillations emerge with the introduction of noise only (no periodic input) into an otherwise nonoscillatory system. It was first reported in a numerical study of a two-dimensional autonomous system [1], whose deterministic behavior is characterized by two stable equilibria separated in its circular phase space by two unstable equilibria. If the system is perturbed beyond the threshold distance between neighboring stable equilibria, the system evolves from one to the other. Similar noisy behavior has been observed in excitable systems, such as the FitzHugh-Nagumo (FHN) [2] and Hodgkin-Huxley (HH) [3] models. There the deterministic systems have a single stable equilibrium, but large "excited" excursions occur for perturbations beyond a threshold. In [2], the term coherence resonance (CR) was introduced to emphasize the fact that relatively coherent oscillations occur at moderate noise levels in such excitable systems. In all of these settings higher noise levels increase the frequency of transitions or excursions, providing the intuition behind a phase plane analysis [4] and the relative first passage time [2] used to explain the increased frequency of the noise-induced coherent oscillations.

These studies have two important characteristics of CR in common. First, the coherence of the dynamics, defined as [1]

$$\beta = h_p(\Delta\omega/\omega_p)^{-1}, \tag{1}$$

reaches a maximum at an optimal level of noise. Here h_p and $\Delta\omega$ are the height and the width of the averaged spectrum peak at frequency ω_p. Second, the frequency of the coherent oscillations depends on the noise level. A large number of studies of noise-induced synchrony in networks of coupled excitable systems, including coupled integrate-and-fire models [5], FHN models [6], HH models [3], and bursting models [7,8] also illustrate these characteristics of CR. Optimal coherence at a finite noise level was explained by Wiesenfeld [9] who revealed how the noise controls the structure of the power spectrum. Similarly, [10] used logistic maps to explain the peak values in the coherence measure.

These earlier results examined CR for oscillations composed of transitions between steady equilibria, where the frequency naturally increases with noise level. In other contexts, the relationship between frequency and noise may vary. For parameter values that are close to a saddle-node point in the periodic branch in the HH model [11], noise variation gives little or no change in the frequency of the coherent oscillations. Instead noise apparently "shifts" the bifurcation structure, yielding stable large amplitude oscillations associated with solution branches far from the Hopf point. Similarly in a network of resonance integrate-and-fire oscillators [8], the noise induces synchronized burst firing in a subthreshold regime, with the frequency of the network oscillations determined by the intrinsic properties of the neurons rather than the noise level. CR is also observed in transitions between steady state and oscillatory modes, [1], [12–17]. There the relationship between the resonance frequency and the noise level depends on the model type. Although all of the cases of CR cited above differ in certain ways, they share the common feature that moderate levels of noise can induce coherent oscillations in a system that is nonoscillatory in the absence of noise. We shall use the term CR to refer to all such phenomena. This includes the case that we study in this paper, although the mechanism for CR is not exactly the same as in the other studies cited above.

In this paper we focus on CR via the canonical model for a normal form near a Hopf bifurcation with additive noise,

$$dx = [(\lambda + \alpha r^2 + \gamma r^4)x - (\omega_0 + \omega_1 r^2)y]dt + \delta_1 d\eta_1(t),$$

$$dy = [(\omega_0 + \omega_1 r^2)x + (\lambda + \alpha r^2 + \gamma r^4)y]dt + \delta_2 d\eta_2(t),$$

$$r^2 = x^2 + y^2, \tag{2}$$

where η_1 and η_2 are independent standard Brownian motions (SBMs). This model captures the generic behavior of excitable systems near a Hopf point $\lambda = 0$. For any specific physical or biological model involving two variables, explicit analytical expressions of the parameters that appear in this normal form can be derived as functions of realistic model parameters for that particular system [18,19].

In the absence of noise, all periodic solutions of this model that bifurcate from the Hopf point are circles that are centered at the origin. The parameters λ, α, and γ determine the dynamics of the amplitude, with α and γ governing the

*Corresponding author: Email address: rachel@math.ubc.ca

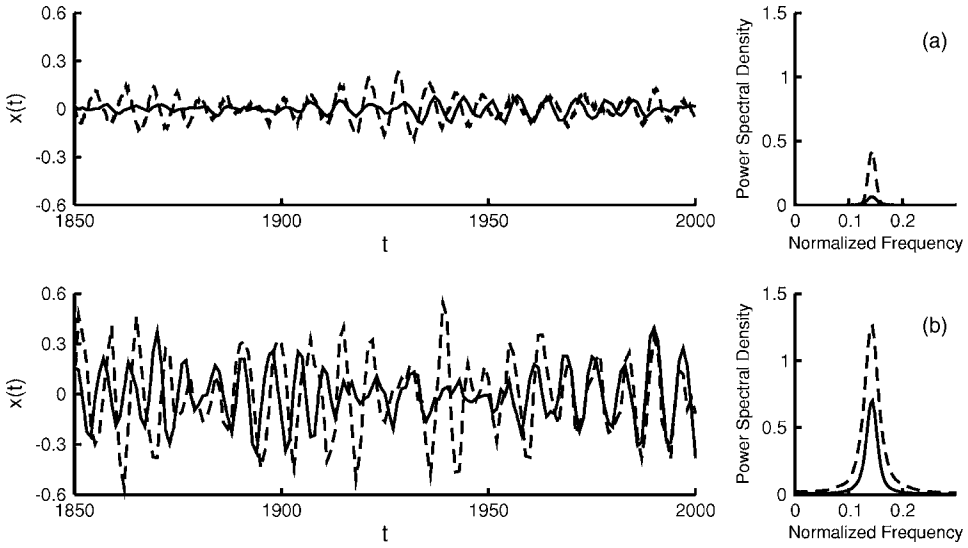

FIG. 1. The amplitude of coherent oscillations in (2) increases as the control parameter $\lambda \to 0$ and as the noise intensity δ increases, while the frequency is concentrated at a single value. The left column shows the time series for $x(t)$ for $\delta_1 = \delta_2 = \delta$. The right column shows the corresponding PSD. For both (a) and (b), the parameters in (2), $\alpha = -0.2, \gamma = -0.2, \omega_0 = 0.9, \omega_1 = 0$, are the same. In (a) $\delta = .01$, $\lambda = -0.03$ (solid line) and $\lambda = -0.003$ (dashed line). In (b) $\lambda = -0.03$, $\delta = 0.07$ (solid line) and $\delta = 0.1$ (dashed line). Recall $\lambda = \epsilon^2 \lambda_2$, which measures distance from the Hopf point.

bifurcation structure away from the Hopf point, while the parameters ω_0 and ω_1 govern the phase dynamics. In particular, the sign of ω_1 determines whether the angular frequency is increased or decreased when the amplitude of the oscillation increases.

We present explicit analytical results in the context where the system parameters approach the bifurcation point so that $|\lambda| \ll 1$. This is a noise-sensitive regime, well known from computations that exhibit CR [16,17]. We begin with (2) for $\alpha < 0$ and $\gamma < 0$, so that $\lambda = 0$ is a supercritical Hopf bifurcation point in the absence of noise. That is, for $\delta_1 = \delta_2 = 0$ the oscillations decay over time for $\lambda < 0$, and oscillations with amplitude r_0 and phase $\Phi = (\omega_0 + \omega_1 r_0^2)t$ are stable for $\lambda > 0$. The parameter ω_1 is an important link between the amplitude and phase; different signs of ω_1 represent different model types with different phase dynamics. In this paper we restrict our attention to $\lambda < 0$, corresponding to a quiescent regime in the absence of noise.

Figure 1 shows a time series with small additive white noise, $0 < \delta_1 = \delta_2 = \delta \ll 1$ and $|\lambda| \ll 1$. The variance of the amplitude of the slowly modulated oscillations increases with δ and as $|\lambda| \to 0$, that is, approaching the Hopf point at $\lambda = 0$. A strong peak in the power spectral density (PSD) indicates a dominant frequency due to CR. This response is induced by the noise since, without noise, the oscillations decay for $\lambda < 0$. There is also a slow phase variation (not apparent on the graphs). Through CR the system exhibits oscillations in this regime, and the analysis reveals the dependence of the phase and amplitude on both the noise level and the model parameters, providing critical scaling relationships related to resonance.

The key to our results is a stochastic multiple scales expansion which exploits the resonance phenomenon in order to derive effective amplitude and phase equations. It is based on the method of multiple scales, commonly used to derive amplitude or evolution equations for deterministic systems in parameter regimes near a bifurcation point [18,19]. The stochastic nature of the model does not allow a standard application of the multiple-scales expansion, so we use a modified approach which incorporates Ito calculus and the properties of the noise [20] into the multiscale approximation. Since the deterministic and stochastic elements of the analysis are well known by themselves, we do not discuss these elements individually but rather focus our discussion on the combination of these approaches for deriving stochastic phase and amplitude equations. Similar approaches have recently been used to derive amplitude equations for the stochastic van der Pol-Duffing (vdPD) equation with both additive [21,22] and multiplicative noise [21], and for stochastic delay differential equations near a critical delay corresponding to a Hopf bifurcation [23].

Here we focus on the stochastic phase dynamics, deriving analytical quantities such as moments for the amplitude and phase, which illustrate the model dependency of the stochastic phase behavior and the noise-amplification factor related to the Hopf bifurcation. In addition these quantities compare well with numerical simulations and provide complementary quantitative insight into the stochastic resonance-type maximum in the numerically computed coherence measure β defined in (1). Computed coherence measures are commonly used as indicators of CR, while the more desirable analytical expressions for the stochastic phase dynamics, derived directly from the model, are rare.

II. ANALYSIS AND RESULTS

We derive a reduced system of stochastic equations for the amplitude and phase of the oscillations described by (2). The derivation uses the method of multiple scales modified appropriately for stochastic systems in which the standard rules of calculus do not apply. The multiscale analysis exploits the fact that the system is near critical in the noise-sensitive regime for $|\lambda| \ll 1$ shown in Fig. 1. That is, the parameters are close to the Hopf point so we can express $\lambda = \epsilon^2 \lambda_2 + O(\epsilon^4)$ with $\epsilon \ll 1$ and $\lambda_2 = O(1) < 0$ for $\lambda < 0$. For deterministic models in this regime, it is well known that the system varies on a slow time scale $T = \epsilon^2 t$, in addition to the original time scale t. Then it is not unexpected that the stochastic system shows a similar multiscale behavior, particularly if the noise is not too large. Indeed, this behavior ap-

pears in simulations shown in Fig. 1, where there is a variation of the amplitude which is slow relative to the t scale. An important ingredient in analyzing these slow modulations is the projection of the system onto the resonant modes which oscillate on the fast time scale. In deterministic systems this projection leads to amplitude equations on a slow time scale, equivalent to an averaging which eliminates (unphysical) secular terms which grow linearly in time [18]. In the stochastic system the projection plays a similar role, producing stochastic amplitude and phase equations with an appropriate approximation for the noisy excursions on the slow time scale [21,23].

To express the behavior on multiple time scales, we allow $x(t,T)$ and $y(t,T)$ to be functions of both time scales t and $T=\epsilon^2 t$,

$$x = \epsilon A(T)\cos(\omega_0 t) - \epsilon B(T)\sin(\omega_0 t),$$

$$y = \epsilon A(T)\sin(\omega_0 t) + \epsilon B(T)\cos(\omega_0 t). \tag{3}$$

The multiscale form of the ansatz for x and y is identical to that used in the leading order approximation for a deterministic system near a Hopf point [18]. The difference here is that A and B must capture the stochastic behavior, with the form (3) appropriate in situations where the noise is small and does not dominate the dynamics. We look for stochastic amplitude equations on the slow time scale for $A(T)$ and $B(T)$ of the form

$$dA = \psi_A dT + \sigma_{A1} d\xi_{11}(T) + \sigma_{A2} d\xi_{12}(T)$$

$$dB = \psi_B dT + \sigma_{B1} d\xi_{21}(T) + \sigma_{B2} d\xi_{22}(T), \tag{4}$$

where $\xi_{ij}(T)$ are independent SBMs on the slow time scale T.

Once we have the equations for A and B, we can obtain the stochastic amplitude R and phase ϕ in terms of A and B, using

$$x = \epsilon R(T)\cos[\omega_0 t + \phi(T)],$$

$$y = \epsilon R(T)\sin[\omega_0 t + \phi(T)], \tag{5}$$

$$R^2 = A^2 + B^2, \quad \phi = \tan^{-1} B/A. \tag{6}$$

The coefficients ψ_A, ψ_B, σ_{Aj}, σ_{Bj} are derived through the multiscale analysis. This derivation stands in contrast to a deterministic analysis where one uses a perturbation expansion following the replacement of x_t with $x_t+\epsilon^2 x_T$ and similarly for y_t. In the general setting of stochastic nonlinear dynamics this multiscale version of the chain rule cannot be directly applied. Instead, we seek the equations for the slow dynamics through the introduction of an appropriate ansatz (4), which is verified by the following derivation of the coefficients; if this ansatz is incorrect, the derivation will show inconsistencies [21,23].

The coefficients in (4) are found from equating expressions for dx and dy obtained by two methods. First, using Ito's formula, which can be viewed as the stochastic version of the chain rule, we relate (2) on the fast time scale to (4) on the slow time scale through (3) and (6) to get

$$dx = \frac{\partial x}{\partial t}dt + \frac{\partial x}{\partial A}dA + \frac{\partial x}{\partial B}dB = -\epsilon[A(T)\omega_0 \sin\omega_0 t + B(T)\omega_0 \cos\omega_0 t]dt + \epsilon\cos\omega_0 t(\psi_A dT + \sigma_{A1}d\xi_{11} + \sigma_{A2}d\xi_{12}) - \epsilon\sin\omega_0 t(\psi_B dT + \sigma_{B1}d\xi_{21} + \sigma_{B2}d\xi_{22}), \tag{7}$$

$$dy = \frac{\partial y}{\partial t}dt + \frac{\partial y}{\partial A}dA + \frac{\partial y}{\partial B}dB = \epsilon[A(T)\omega_0 \cos\omega_0 t - B(T)\omega_0 \sin\omega_0 t]dt + \epsilon\sin\omega_0 t(\psi_A dT + \sigma_{A1}d\xi_{11} + \sigma_{A2}d\xi_{12}) + \epsilon\cos\omega_0 t(\psi_B dT + \sigma_{B1}d\xi_{21} + \sigma_{B2}d\xi_{22}). \tag{8}$$

Note that, in general, Ito's formula would include terms consisting of the second derivatives of x and y with respect to A and B with coefficients involving σ_{ij}, but these terms vanish due to the linear relationship between x and y with A and B in (3). Secondly, by direct substitution of (3) and (6) into the original equations (2), we get

$$dx = [\epsilon^3(\lambda_2 + \alpha R^2 + \epsilon^2\beta R^4)(A\cos\omega_0 t - B\sin\omega_0 t) - (\epsilon\omega_0 + \epsilon^3\omega_1 R^2)(A\sin\omega_0 t + B\cos\omega_0 t)]dt + \delta_1 d\eta_1, \tag{9}$$

$$dy = [(\epsilon\omega_0 + \epsilon^3\omega_1 R^2)(A\cos\omega_0 t - B\sin\omega_0 t) + \epsilon^3(\lambda_2 + \alpha R^2 + \epsilon^2\beta R^4)(A\sin\omega_0 t + B\cos\omega_0 t)]dt + \delta_2 d\eta_2. \tag{10}$$

Now we set (7) and (8) equal to (9) and (10), respectively. The first steps in the calculation are shown in the Appendix: collecting coefficients of like powers of ϵ, the $O(\epsilon)$ terms cancel, since (3) are solutions to the linearized system with A and B treated as constants with respect to the original time scale. When written in terms of this fast time scale t, the leading order nonzero contribution to the drift terms is $O(\epsilon^3)$ and the leading order contributions to the noise terms have coefficients δ_1, δ_2 in (A1) and (A2). By considering these terms together as the leading order nontrivial contributions, we have implicitly assumed that $\delta_j < \epsilon$. The ansatz (3) in the form of the solution of the linearized noise-free system is also implicitly based on this assumption, which is discussed further below in the context of the validity of the multiscale approximation.

Since the goal is to derive the coefficients in the stochastic amplitude equations (4), we rewrite the leading order terms from (A1) and (A2) on the slow time scale T,

$$\cos\omega_0 t(\psi_A dT + \sigma_{A1}d\xi_{11} + \sigma_{A2}d\xi_{12}) - \sin\omega_0 t(\psi_B dT + \sigma_{B1}d\xi_{21} + \sigma_{B2}d\xi_{22}) = [\sin\omega_0 t(-\lambda_2 B - \omega_1 R^2 A - \alpha R^2 B) + \cos\omega_0 t(\lambda_2 A - \omega_1 R^2 B + \alpha R^2 A)]dT + \frac{\delta_1}{\epsilon}d\eta_1 \tag{11}$$

and

$$\sin\omega_0 t(\psi_A dT + \sigma_{A1} d\xi_{11} + \sigma_{A2} d\xi_{12}) + \cos\omega_0 t(\psi_B dT + \sigma_{B1} d\xi_{21} + \sigma_{B2} d\xi_{22}) = [\sin\omega_0 t(\lambda_2 A - \omega_1 R^2 B + \alpha R^2 A) + \cos\omega_0 t(\lambda_2 B + \omega_1 R^2 A + \alpha R^2 B)]dT + \frac{\delta_2}{\epsilon} d\eta_2. \quad (12)$$

These expressions involve oscillations ($\cos\omega_0 t$ and $\sin\omega_0 t$) on the fast time scale t, and coefficients involving A, B, ψ_A, and ψ_B which depend on the slow time T. To separate the slow time behavior, we project (11) and (12) onto the primary mode of oscillations with frequency ω_0 on the time scale t. Combined with the multiscale assumptions which treat functions of T as independent of t, this projection leaves terms which depend on T only, thus yielding equations for ψ_A, ψ_B, and σ_{Aj}, σ_{Bj}, $j=1,2$ in (4). This projection is identical to the solvability condition used in normal form calculations [18,19] to eliminate secular terms, and has the form

$$\int_0^{2\pi/\omega_0} (\cos\omega_0 t, \sin\omega_0 t)\cdot[\text{Eqs. (11),(12)}]dt,$$

$$\int_0^{2\pi/\omega_0} (-\sin\omega_0 t, \cos\omega_0 t)\cdot[\text{Eqs. (11),(12)}]dt. \quad (13)$$

Under the multiscale assumption, those functions of the slow time T in (13) are treated as constants in the integration. Since the periodic behavior in the system (2) can be expressed in terms of trigonometric functions, the integrals in (13) can be computed analytically. In other situations where the periodic behavior is expressed in terms of more complicated functions or a limit cycle, the projection has to be done numerically. Nevertheless the procedure is similar in this more general case, as shown, for example, in [24]. For simplicity of presentation, we write the results of the projection in terms of the drift and diffusion terms separately.

The drift terms are

$$\begin{pmatrix} \cos\omega_0 t & -\sin\omega_0 t \\ \sin\omega_0 t & \cos\omega_0 t \end{pmatrix}\begin{pmatrix} \psi_A \\ \psi_B \end{pmatrix} dT = \begin{pmatrix} \cos\omega_0 t & -\sin\omega_0 t \\ \sin\omega_0 t & \cos\omega_0 t \end{pmatrix}\begin{pmatrix} \lambda_2 A + R^2(\alpha A - \omega_1 B) \\ \lambda_2 B + R^2(\alpha B + \omega_1 A) \end{pmatrix} dT. \quad (14)$$

We get ψ_A and ψ_B by using (13) and integrating over one period of the oscillation of length $2\pi/\omega_0$ on the t time scale,

$$\int_0^{2\pi/\omega_0} (\cos\omega_0 t, \sin\omega_0 t)\cdot[\text{Eq. (14)}]dt \Rightarrow \psi_A = \lambda_2 A + R^2(\alpha A - \omega_1 B),$$

$$\int_0^{2\pi/\omega_0} (-\sin\omega_0 t, \cos\omega_0 t)\cdot[\text{Eq. (14)}]dt \Rightarrow \psi_B = \lambda_2 B + R^2(\alpha B + \omega_1 A). \quad (15)$$

We give some details here for the derivation of the diffusion (noise) coefficients in (4). Before applying the projection, we use the properties of white noise to express all of the noise terms on the slow time scale T and to write $d\eta_j$ in a form that captures explicitly the contribution of the primary oscillatory modes,

$$\begin{pmatrix} d\eta_1 \\ d\eta_2 \end{pmatrix} = \epsilon^{-1}\begin{pmatrix} \cos\omega_0 t d\eta_{A1}(T) - \sin\omega_0 t d\eta_{B1}(T) \\ \sin\omega_0 t d\eta_{A2}(T) + \cos\omega_0 t d\eta_{B2}(T) \end{pmatrix} \quad (16)$$

with η_{Aj} and η_{Bj} independent SBMs for $j=1,2$. Then the noise terms in (11) and (12) are

$$\epsilon\begin{pmatrix} \cos\omega_0 t & -\sin\omega_0 t \\ \sin\omega_0 t & \cos\omega_0 t \end{pmatrix}\begin{pmatrix} \sigma_{A1} d\xi_{11} + \sigma_{A2} d\xi_{12} \\ \sigma_{B1} d\xi_{21} + \sigma_{B2} d\xi_{22} \end{pmatrix} = \frac{1}{\epsilon}\begin{pmatrix} \delta_1(\cos\omega_0 t d\eta_{A1}(T) - \sin\omega_0 t d\eta_{B1}(T)) \\ \delta_2(\sin\omega_0 t d\eta_{A2}(T) + \cos\omega_0 t d\eta_{B2}(T)) \end{pmatrix}. \quad (17)$$

To obtain $\sigma_{A1}, \sigma_{A2}, \sigma_{B1}$, and σ_{B2}, we again use the projection as in (15); we project (17) onto the primary modes,

$$\int_0^{2\pi/\omega_0} (\cos\omega_0 t, \sin\omega_0 t)\cdot[\text{Eq. 17}]dt \Rightarrow \sigma_{A1} d\xi_{11} + \sigma_{A2} d\xi_{12} = \frac{\delta_1}{2\epsilon^2} d\eta_{A1} + \frac{\delta_2}{2\epsilon^2} d\eta_{A2}, \quad (18)$$

$$\int_0^{2\pi/\omega_0} (-\sin\omega_0 t, \cos\omega_0 t)\cdot[\text{Eq. 17}]dt \Rightarrow \sigma_{B1} d\xi_{21} + \sigma_{B2} d\xi_{22} = \frac{\delta_1}{2\epsilon^2} d\eta_{B1} + \frac{\delta_2}{2\epsilon^2} d\eta_{B2} \quad (19)$$

The multiscale ansatz is also applied, treating functions of the slow time T as independent of the fast time t. This yields

$$\sigma_{A1} d\xi_{11} + \sigma_{A2} d\xi_{12} = d\zeta_A/(2\epsilon^2),$$

$$\sigma_{B1} d\xi_{21} + \sigma_{B2} d\xi_{22} = d\zeta_B/(2\epsilon^2), \quad (20)$$

where $d\zeta_m = \delta_1 d\eta_{m1} + \delta_2 d\eta_{m2}$, $m=A,B$. Identifying the appropriate relationships between the SBM's, we let $\xi_{11}=\eta_{A1}$, $\xi_{12}=\eta_{A2}$, $\xi_{21}=\eta_{B1}$, and $\xi_{22}=\eta_{B2}$, which yields

$$\sigma_{A1} = \frac{\delta_1}{2\epsilon^2}, \quad \sigma_{A2} = \frac{\delta_2}{2\epsilon^2}, \quad \sigma_{B1} = \frac{\delta_1}{2\epsilon^2}, \quad \sigma_{B2} = \frac{\delta_2}{2\epsilon^2}. \quad (21)$$

Note that in the use of the projection above, we have treated white noise on the T time scale as if it is independent of the fast t scale; of course, since white noise contains fluctuations on all time scales, this assumption is not true, in general. Nevertheless, the application of the projection yields an appropriate approximation for the noise in the amplitude equations. This reflects the fact that if one used a full Fourier-type expansion for x and y [25], then the amplitudes of the additional modes beyond those shown in (3) would decay exponentially on the time scale t [23]. Treating the noise as independent of the fast time scale reflects the decay of these additional modes of oscillation on this scale.

The diffusion terms in the amplitude equations for the stochastic vdPD equation have been derived in [21] using Ito's formula together with the projection method discussed

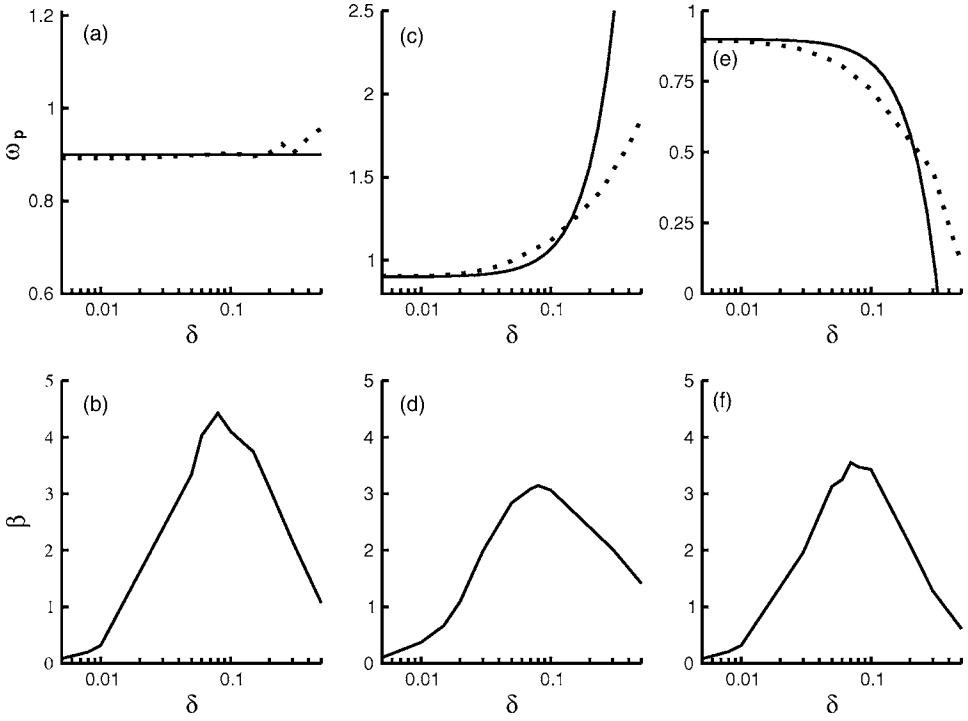

FIG. 2. The behavior of the peak frequency from the PSD and the numerically computed coherence measure β are shown as functions of the noise. For all figures, the control parameter is $\lambda = -0.03$, the noise level is $\delta_1 = \delta_2 = \delta$, and the other parameters in (2) are $\alpha = -0.2$, $\gamma = -0.2$, and $\omega_0 = 0.9$. Upper: peak frequency ω_p of the PSD peak vs the noise intensity for $\omega_1 = 0$ in (a) $\omega_1 = 1.2$ in (c), and $\omega_1 = -0.5$ in (e). The solid line gives the asymptotic results (27) and the dotted line gives numerical results. Lower: coherence measure β vs δ. The parameters in (b), (d), and (f) match those in (a), (b), and (c), respectively.

above, while in [22] the root mean square of $\cos \omega_0 t$ and $\sin \omega_0 t$ were used in an approximation of the effective diffusion coefficient. In these studies the factor ϵ^{-1} appears as an amplification factor in the noise coefficients for reduced equations on the slow time scale T, as in (21).

From (6), (4), (15), and (20) and using Ito's formula again, we then obtain the equations for the stochastic amplitude and phase, as shown in the Appendix,

$$dR^2 = [2R^2(\lambda_2 + \alpha R^2) + \Delta]dT + R[\cos \phi \, d\zeta_A + \sin \phi \, d\zeta_B]/\epsilon^2, \tag{22}$$

$$d\phi = R^2 \omega_1 dT + (\cos \phi \, d\zeta_B - \sin \phi \, d\zeta_A)/(2\epsilon^2 R), \tag{23}$$

where $\Delta = (\delta_1^2 + \delta_2^2)/(2\epsilon^4)$. From (22) and (23), we obtain the differential equations for the expected values of R^2 and ϕ

$$d(E[R^2]) = E[d(R^2)] = [2\lambda_2 E[R^2] + 2\alpha E[R^4] + \Delta]dT, \tag{24}$$

$$d(E[\phi]) = E[d\phi] = E[R^2]\omega_1 dT. \tag{25}$$

Using an asymptotic expansion for small Δ, we get the leading order steady state results for the moments by neglecting $E[R^4]$ in (24) and (25), which is a higher order correction as shown in the Appendix. Then to leading order we have

$$E[R^2] \sim -\frac{\Delta}{2\lambda_2}, \tag{26}$$

$$E[\phi] \sim -\frac{\Delta}{2\lambda_2}\omega_1 T + \psi_0, \tag{27}$$

omitting higher order corrections with coefficient Δ^2 (see Appendix). Here ψ_0 is a constant phase shift, which can be set to zero. Below we discuss that this asymptotic expansion is consistent with $r^2 = \epsilon^2 R^2 = O(\delta_j^2/\epsilon^2)$, with δ_j/ϵ small.

The expected phase $E[\phi]$ depends on the noise through the term $R^2\omega_1 dT$ in (23), giving the phase behavior shown in Fig. 2. In the top row we compare the numerical and analytical results for the expected value for the frequency associated with the peak of the PSD; that is, it is the coherence frequency induced by the resonance with the noise. The analytical results are obtained using (27), while the numerical results are obtained from the averaged PSD over a large number (1200) of realizations of the original system (2). Figure 2 shows a good agreement between simulations and analysis for $\delta/\epsilon < 1$. For $\omega_1 = 0$, the expected value of the phase does not depend on the noise, while for $\omega_1 > (<) 0$, the coherence frequency increases (decreases) with the noise. The results are shown for symmetric noise ($\delta_1 = \delta_2 = \delta$), and a similar behavior is observed for $\delta_1 \neq \delta_2$.

Figure 2 (bottom row) gives the numerically computed coherence measure β. It is obtained using the averaged PSD for (2), using the shape of the frequency peak to compute β in (1). The graphs show roughly the same behavior for β for vanishing, positive, and negative values of ω_1 which characterizes the model type. For $\delta_1 = \delta_2 = \delta$ near 0, β is small, followed by a sharp increase to its maximum for values $0 < \delta < 0.1$ and decreasing β for $\delta > 0.1$.

While β gives a measure of the coherence, it does not provide any details about the phase. For example, from β we cannot conclude whether the average frequency is increasing or decreasing with noise. The analytical results (22)–(27) give a complete description of the stochastic behavior of the amplitude and phase behavior, both in terms of the noise level and the model parameters, providing a view beyond the numerical results of β. For example, we get the quantitative relationships for the dependence of the phase on ω_1 and δ_j as well as explicit expressions for the amplification factors near

the Hopf point, which cannot be obtained by computing β.

The analytical result provides information about the coherence, similar to that given by the numerical calculation of β, but this coherence information does not come from the calculation of the same quantities that appear in the definition of β. In particular, the width of the PSD ($\Delta\omega$) cannot, in general, be computed analytically using this multiscale approach. Rather, the coherence information from the analytical results follows from a consideration of the validity of the approach. The multiscale analysis is valid for noise levels that do not overwhelm the resonant oscillations. In order to quantify this statement, the stochastic amplitude equation (22) is written in terms of the amplitude $r=\epsilon R$ from the single mode approximation (3), yielding

$$dr^2 = [2r^2(\lambda_2 + \alpha r^2/\epsilon^2) + \epsilon^2\Delta]dT + r[\cos\phi\, d\zeta_A + \sin\phi\, d\zeta_B]/\epsilon. \quad (28)$$

This rescaling shows that the noise coefficient in the equation for the unscaled amplitude is $O(\delta_j/\epsilon)$ since $\zeta/\epsilon = O(\delta_j/\epsilon)$ (20), and it is this coefficient which indicates the balance between the noise and the oscillations. While the term r^4/ϵ^2 appears to be large, in fact, given the exponential decay of the deterministic part and small noise, this term does not dominate the dynamics for CR. Thus the quantitative results give the asymptotic range for the coherence effect in terms of the parameters for the noise level δ_j and proximity to criticality ϵ. For $\delta_j/\epsilon = o(1)$ the noise does not dominate the dynamics, allowing coherent oscillations whose amplitude r increases with both increasing noise level δ_j and decreasing distance ϵ from the bifurcation point. For larger values of $\delta_j/\epsilon > 1$, the noise in (28) is large, altering the dynamics qualitatively by introducing additional modes into the oscillatory behavior, so that the single mode approximation (3) breaks down.

This validity regime for the asymptotic results can be related to the behavior of β by first noting that the amplitude r is related to the numerator for the coherence measure β as

$$h_p = O(|r|) = O(\delta_j/\epsilon). \quad (29)$$

For very small δ_j/ϵ, (22) and (29) show that the resonant oscillation is present with small power, so that β is small using (29) in (1). For increasing $\delta_j/\epsilon < 1$ this amplitude is increased so that β increases, with (3) still a valid approximation. For $\delta_j/\epsilon = O(1)$ or larger, (3) is less accurate since the larger noise supports additional modes which then cannot be neglected in the approximation [23]. Due to the contributions of these other modes, $|x(t) - \epsilon R\cos(\omega_0 t + \phi)|$ increases as does the width of the PSD peak. That is, the variation of x and y from (3) for $\delta_j/\epsilon = O(1)$ or larger is mirrored in the denominator $\Delta\omega/\omega_p$ of β but not in the numerator (29). Therefore the loss of coherence for $\delta_j/\epsilon = O(1)$ or larger is reflected both in the breakdown of the approximation (3) and the decrease of β which is computed numerically.

III. SUMMARY AND EXTENSIONS

A stochastic multiple-scales method yields analytical quantities for the stochastic amplitude and phase for an oscillator exhibiting CR near a Hopf bifurcation. Explicit expressions show how the phase and amplitude dynamics depend on the model, providing additional information beyond numerically computed coherence measures. Phase variations due to the noise level and model type are characterized by a parameter ω_1 which captures the coupling between the phase and amplitude. The phase behavior differs from the increased coherence frequency typically observed in systems with a threshold. The amplification of the oscillations is related to the proximity to criticality measured by ϵ.

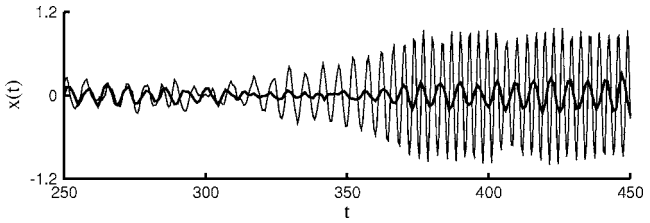

FIG. 3. Time series for the subcritical case, taking $\alpha=0.2$, $\gamma=-0.2, \omega_0=0.9$, and $\omega_1=1.2$ in (2), with control parameter $\lambda=-0.03$. The noise levels are $\delta=0.02$ (bold line) and $\delta=0.04$ (thin line). Even though the noise levels for both are $O(|\lambda|)=O(\epsilon^2)$, the variance of the amplitude for larger values of δ is sufficiently large to cause a transition to a state with $O(1)$ oscillations.

This derivation of stochastic amplitude equations (4) has been used in applications where autonomous stochastic resonance appears due to noise sensitivity (see [23], and references therein). A key component is the projection onto the primary modes combined with the multiscale ansatz. While it is true that the noise is white with all frequency components, this projection selects out the components corresponding to the resonant mode which do not decay exponentially over long time scales. Then the primary mode dominates the dynamics through CR over a long time scale (4), while the other modes decay at a sufficiently fast rate to be of higher order for $\delta \ll \epsilon$. Note that on the long time scale, the noise has an additional factor of ϵ^{-1}, corresponding to the amplification of the oscillations.

Extensions of the analysis are particularly valuable in noise-sensitive systems where computations can be delicate or expensive. Stochastic phase and amplitude equations were derived for the relaxation oscillations of an elliptic burster in [24], and we mention two important problems related to (2) for which we have preliminary results.

1. *Transitions from steady state to large amplitude oscillations in the context of subcritical bifurcations*. This phenomenon occurs when $\alpha > 0$ and $\beta < 0$ in (2), so that there is a stable bifurcation branch of oscillatory solutions with a large amplitude. Small perturbations or oscillations decay to zero in the absence of noise since small amplitude oscillations are unstable. However, larger perturbations trigger jumps to the stable large amplitude oscillations. The probability or expected time of this transition is directly related to the amplitude $E[R]$, derived from (23)–(27). In Fig. 3 the transition to a large amplitude is highly improbable for small enough noise ($\delta=.02$) (bold line), but it can occur for noise levels which are increased by a factor of 2 (thinner line), but are still the same order of magnitude as in the case where the transition does not occur. A similar phenomenon is observed if λ approaches the critical Hopf point.

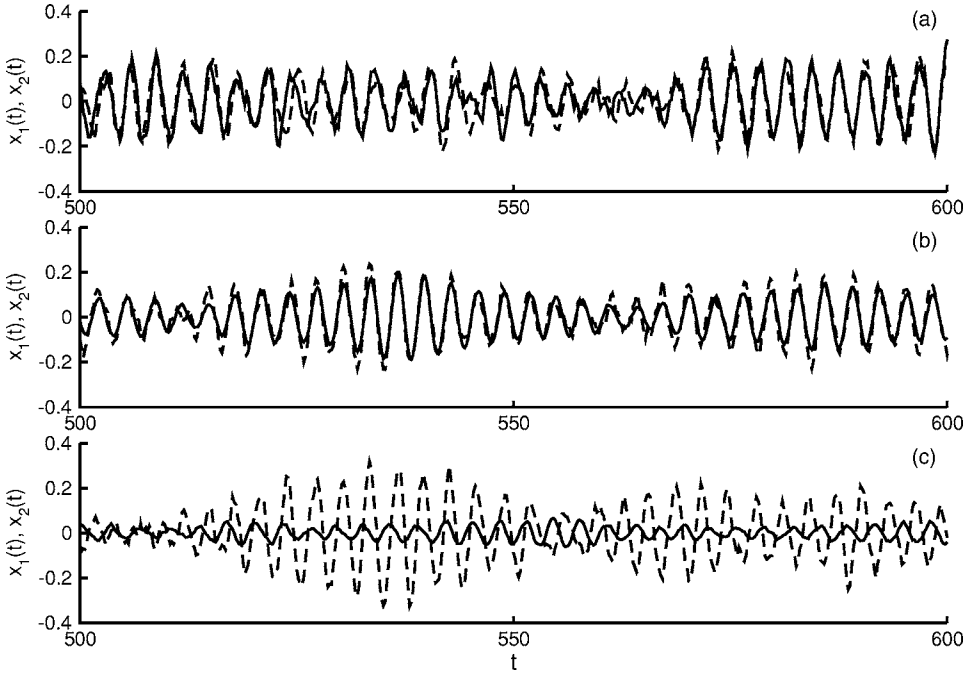

FIG. 4. Time series for diffusively coupled systems of the type (2) when the control parameter for each is $\lambda=-0.03$ and the other parameters are $\alpha=-0.2$, $\gamma=-0.2, \omega_0=2$, and $\omega_1=1$, starting with small initial conditions, illustrating different effects of the interaction of noise and coupling. Solid and dashed lines are for $x(t)$ in the first and second oscillators, respectively. (a) and (b) the coupling strength is $d=0.05$, while in (a) the noise levels are identical $\delta_1=0.05$, $\delta_2=0.05$ and in (b) the noise level of the first oscillator is reduced $\delta_1=0.01$, $\delta_2=0.05$. In (c) the noise levels are the same as in (b), but the coupling is reduced, $d=0.001$.

2. *Interaction and competition between coupling and noise in systems near critical*. We consider numerically two diffusively coupled oscillators of the form (2), observing results in Fig. 4 which show an interplay between noise and coupling in synchronization, suggesting future directions for the study of stochastic effects on the amplitude and phase. The (top) figure shows intermittency between periods of phase locking and phase drifts for noise and coupling at the same strength. In the middle graph the noise in one of the oscillators is reduced, keeping all other parameters the same as the top graph, and the synchronization appears to be strengthened, even though the noise levels are asymmetric. In the bottom graph, where the coupling is smaller than in the top and middle graphs and the noise levels are asymmetric, the signals look dissimilar in amplitude and phase. Preliminary results indicate that in these parameter ranges it is possible to use a similar multiscale analysis to derive the coupled slowly varying stochastic phase and amplitude equations. Through CR the amplification of the noise depends on ϵ^{-1}, and contributions from the coupling are similarly amplified. The goal of this future work is to be able to obtain explicit parameteric results for the stochastic phase and amplitude in the coupled case, leading to effective definitions which can be compared to commonly used numerical measures.

APPENDIX

The equation obtained by equating the expressions (7) and (9) for dx is

$$[-(A(T)\omega_0\sin\omega_0 t + B(T)\omega_0\cos\omega_0 t)dt]\epsilon dt + \epsilon[\cos\omega_0 t(\psi_A dT + \sigma_{A1}d\xi_{11} + \sigma_{A2}d\xi_{12}) - \sin\omega_0 t(\psi_B dT + \sigma_{B1}d\xi_{21} + \sigma_{B2}d\xi_{22})]$$
$$= \{-\epsilon\omega_0(A\sin\omega_0 t + B\cos\omega_0 t) + \epsilon^3[\sin\omega_0 t(-\lambda_2 B - \omega_1 R^2 A - \alpha R^2 B) + \cos\omega_0 t(\lambda_2 A - \omega_1 R^2 B + \alpha R^2 A)]\}dt + O(\epsilon^5) + \delta_1 d\eta_1, \tag{A1}$$

and equating (8) and (10) for dy we get

$$\{[A(T)\omega_0\cos\omega_0 t - B(T)\omega_0\sin\omega_0 t]dt\}\epsilon\, dt + \epsilon[\sin\omega_0 t(\psi_A dT + \sigma_{A1}d\xi_{11} + \sigma_{A2}d\xi_{12}) + \cos\omega_0 t(\psi_B dT + \sigma_{B1}d\xi_{21} + \sigma_{B2}d\xi_{22})]$$
$$= \{\epsilon\omega_0(A\cos\omega_0 t - B\sin\omega_0 t) + \epsilon^3[\sin\omega_0 t(\lambda_2 A - \omega_1 R^2 B + \alpha R^2 A) + \cos\omega_0 t(\lambda_2 B + \omega_1 R^2 A + \alpha R^2 B)]\}dt + O(\epsilon^5) + \delta_2 d\eta_2. \tag{A2}$$

Clearly from the above equations, the drift coefficients for the dynamics on the fast scale (appearing with $\epsilon\, dt$) cancel. Note that there are drift coefficients appearing with $\epsilon\, dT$, but these terms are $O(\epsilon^3)$ on the t scale. Then the remaining terms in the x equation on the fast time scale are

$$\cos\omega_0 t(\psi_A dT + \sigma_{A1}d\xi_{11} + \sigma_{A2}d\xi_{12}) - \sin\omega_0 t(\psi_B dT + \sigma_{B1}d\xi_{21} + \sigma_{B2}d\xi_{22})$$
$$= \epsilon^2[\sin\omega_0 t(-\lambda_2 B - \omega_1 R^2 A - \alpha R^2 B) + \cos\omega_0 t(\lambda_2 A - \omega_1 R^2 B + \alpha R^2 A)]dt + \frac{\delta_1}{\epsilon}d\eta_1, \tag{A3}$$

and similarly for the y equation, dropping $O(\epsilon^4)$ terms.

Following the projection onto the fast modes shown in Sec. II, we are left with (15) and the system for the amplitudes A and B,

$$\begin{pmatrix} dA \\ dB \end{pmatrix} = \begin{pmatrix} \lambda_2 A + (\alpha A - \omega_1 B)R^2 \\ \lambda_2 B + (\alpha B + \omega_1 A)R^2 \end{pmatrix} dT + \sigma \begin{pmatrix} d\eta_{A1} \\ d\eta_{A2} \\ d\eta_{B1} \\ d\eta_{B2} \end{pmatrix},$$

$$\text{where} \quad \sigma = \begin{pmatrix} \delta_1/2\epsilon^2 & \delta_2/2\epsilon^2 & 0 & 0 \\ 0 & 0 & \delta_1/2\epsilon^2 & \delta_2/2\epsilon^2 \end{pmatrix}. \quad \text{(A4)}$$

Using Ito's formula again, we write the system (A4) in terms of R^2 and ϕ as

$$\begin{aligned} dR^2 &= \frac{\partial R^2}{\partial A} dA + \frac{\partial R^2}{\partial B} dB + \sum_{m=A,B} \frac{\partial^2 R^2}{\partial m^2} \frac{\sigma_{m1}^2 + \sigma_{m2}^2}{2} dT \\ &= \left[2R^2(\lambda_2 + \alpha R^2) + \frac{\delta_1^2 + \delta_2^2}{2\epsilon^4} \right] dT \\ &\quad + \frac{R}{\epsilon^2} [\cos\phi(\delta_1 d\eta_{A1} + \delta_2 d\eta_{A2}) \\ &\quad + \sin\phi(\delta_1 d\eta_{B1} + \delta_2 d\eta_{B2})]. \end{aligned} \quad \text{(A5)}$$

$$\begin{aligned} d\phi &= \frac{\partial \phi}{\partial A} dA + \frac{\partial \phi}{\partial B} dB + \sum_{m=A,B} \frac{\partial^2 \phi}{\partial m^2} \frac{\sigma_{m1}^2 + \sigma_{m2}^2}{2} dT \\ &= R^2 \omega_1 dT + \frac{1}{2\epsilon^2 R} [\cos\phi(\delta_1 d\eta_{B1} + \delta_2 d\eta_{B2}) \\ &\quad - \sin\phi(\delta_1 d\eta_{A1} + \delta_2 d\eta_{A2})]. \end{aligned} \quad \text{(A6)}$$

With the substitution (20), (A5), and (A6) become the stochastic amplitude and phase equations (22) and (23). In order to get explicit expressions for $E[R^2]$ and $E[\phi]$ we use an asymptotic approximation for small $\Delta = (\delta_1^2 + \delta_2^2)/(2\epsilon^4)$ in their equations (24) and (25). We find that the leading order steady state result for $E[R^2]$ is $-\Delta/2\lambda_2$ by neglecting the $E[R^4]$ terms in (24), and here we show that these correction terms are $O(\Delta^2)$. In particular, using Ito's formula, (A5) and $d\zeta_m = \delta_1 d\eta_{m1} + \delta_2 d\eta_{m2}$ for $m = A, B$,

$$dR^4 = [4\Delta R^2 + 4\lambda_2 R^4 + 4\alpha R^6] + \frac{2R^3}{\epsilon^2} [\cos\phi\, d\zeta_A + \sin\phi\, d\zeta_B], \quad \text{(A7)}$$

$$E[dR^4] = d(E[R^4]) = [4\Delta E[R^2] + 4\lambda_2 E[R^4] + O(R^6)]dT.$$

Then the steady state for $E[R^4]$ can be obtained from (A7)

$$E[R^4] = -\frac{\Delta E[R^2]}{\lambda_2} + O(R^6), \quad \text{(A8)}$$

neglecting terms that decay exponentially. Substituting (A8) into (24), and writing $E[R^2] = -\Delta/2\lambda_2 + \Delta^2 V$ we get a differential equation in terms of V

$$dV = \left(2\lambda_2 V + \frac{\alpha}{\lambda_2^2} \right) dT + O(\Delta), \quad \text{(A9)}$$

and solve it for $V \approx e^{2\lambda_2(T+T_0)} - \alpha/2\lambda_2^3$, where T_0 is the initial time value which can be set to 0. Thus the higher order corrections to $E[R^2]$ are all Δ^2.

[1] Hu Gang, T. Ditzinger, C.-Z. Ning, and H. Haken, Phys. Rev. Lett. **71**, 807 (1993).
[2] A. S. Pikovsky and J. Kurths, Phys. Rev. Lett. **78**, 775 (1997).
[3] Y. Wang, D. T. W. Chik, and Z. D. Wang, Phys. Rev. E **61**, 740 (2000).
[4] W.-J. Rappel and S. H. Strogatz, Phys. Rev. E **50**, 3249 (1994).
[5] W.-J. Rappel and A. Karma, Phys. Rev. Lett. **77**, 3256 (1996).
[6] A. Neiman, L. Schimansky-Geier, A. Cornell-Bell, and F. Moss, Phys. Rev. Lett. **83**, 4896 (1999).
[7] A. Longtin, Phys. Rev. E **55**, 868 (1997).
[8] S. Reinker, Y.-X. Li, and R. Kuske, Bull. Math. Biol. (to be published).
[9] K. Wiesenfeld, J. Stat. Phys. **38**, 1071 (1985).
[10] A. Neiman, P. I. Saparin, and L. Stone, Phys. Rev. E **56**, 270 (1997).
[11] S.-G. Lee, A. Neiman, and S. Kim, Phys. Rev. E **57**, 3292 (1998).
[12] J. Garcia-Ojalvo and R. Roy, Phys. Lett. A **224**, 51 (1996).
[13] S. Kim, S. H. Park, and H. B. Pyo, Phys. Rev. Lett. **82**, 1620 (1999).
[14] T. Ohira and Y. Sato, Phys. Rev. Lett. **82**, 2811 (1999).
[15] A. Beuter, J. Belair, and C. Labrie, Bull. Math. Biol. **55**, 525 (1993).
[16] *Stochastic Dynamics*, edited by H. Crauel and M. Gundlach (Springer-Verlag, New York, 1999).
[17] L. Arnold, N. Sri Namachchivaya, and K. Schenk-Hoppe, Int. J. Bifurcation Chaos Appl. Sci. Eng. **6**, 1947 (1996).
[18] J. Kevorkian and J. D. Cole, *Perturbation Methods in Applied Mathematics* (Springer-Verlag, New York, 1985).
[19] J. C. Neu, SIAM J. Appl. Math. **37**, 307 (1979).
[20] Z. Schuss, *Theory and Applications of Stochastic Differential Equations* (Wiley, New York, 1980).
[21] R. Kuske, in *Nonl. Stoch. Dyn. IUTAM Proc.*, edited by N. Sri Namachchivaya and Y. C. Lin (Kluwer, Dordrecht, 2003).
[22] C. Mayol, R. Toral, and C. R. Mirasso, Phys. Rev. E **69**, 066141 (2004).
[23] M. M. Kłosek and R. Kuske, Multiscale Model. Simul. **3**, 706 (2005).
[24] R. Kuske and S. M. Baer, J. Appl. Math. **64**, 447 (2002).
[25] J.-P. Kahane, *Some Random Series of Functions*, 2nd ed. (Cambridge University Press, Cambridge, UK, 1985).